

Neutral vs Ion Line Widths in the prestellar core L1544

CATALINA V. ZAMORA ¹ AND ANIKA SCHMIEDEKE²

¹*University of Washington, 3910 15th Ave NE, Seattle, WA 98195-1700, USA*

²*Green Bank Observatory, 155 Observatory Road, Green Bank, WV 24944, USA*

ABSTRACT

This report discusses the process of working on my summer project. My project aims to analyze more spectral line data that could potentially corroborate a new hypothesis of molecular behavior in dense cores. I analyzed spectral line observations of the prestellar core L1544, located in the Taurus Molecular Cloud, determined the line widths of the ion N_2H^+ and the neutral NH_3 , and compared the results using a whole host of python-based packages such as SpectralCube, PySpecKit, and APLPy. The report will then discuss the tentative results I determined at the end of my ten-week appointment.

1. INTRODUCTION

I have been looking at ion versus neutral line widths in prestellar core L1544. For this work I have been investigating two different molecular species, namely the ion N_2H^+ and the neutral NH_3 . The ion N_2H^+ is typically used as a dense gas tracer. Its critical density is 10^4 cm^{-3} , while the critical density of the neutral NH_3 is 10^3 cm^{-3} (Shirley 2015). From the empirical line-width-size relationship (Larson 1981; Solomon & Rivolo 1989) one would theoretically expect smaller molecular clouds of higher density being more quiescent. Hence, if this relation holds within individual dense cores, one would expect tracers with higher critical density exhibiting narrower line widths. In the case of the tracers used in this study, the ion N_2H^+ should have narrower line widths than the neutral NH_3 . In addition the ion is expected to be linked to the magnetic field, while the neutral is unaffected by the magnetic field, which means the neutral should be able to move more freely around the core, while the ion is tethered to the magnetic field of the dense core. This also would lead to narrower expected line width for the ion compared to the neutral. However, (Pineda et al. 2021) recently presented opposing results to this theoretical behaviour when analyzing observations of the dense core Barnard 5 (hereafter B5) in the Perseus Molecular Cloud, about 305 parsec away (Zucker et al. 2018). They report wider line widths for the ion N_2H^+ compared to the neutral NH_3 in B5. The distribution of sonic Mach number for B5 from Pineda et al. (2021) depicts the wider line widths in N_2H^+ (see their Fig. 8). The Sonic Mach number is directly related to the non-thermal velocity linewidths, so using the Sonic Mach Number distribution is a good way to compare the widths of the molecules. In addition, other regions have also been reported in the literature to show a similar behaviour (e.g. Tafalla et al. 2004; Sokolov et al. 2019). Unlike B5, which is a multiple system containing a more evolved protostar and multiple starless cores, L1544 is a single prestellar core, which means it is gravitationally bound and on the verge to form a protostar. L1544 is located in the Taurus Molecular cloud about 170 pc away from Earth (Galli et al. 2018). I spent all my time this summer analyzing this core and determining its linewidths in the two tracers, N_2H^+ , and NH_3 .

This report is structured as follows: In Sec. 2 I describe the observational data used in this study. In Sec. 3 I present the methods I employed. In Sec. 4 I present my results and in Sec. 5 I discuss future work.

2. OBSERVATIONS

The N_2H^+ data was obtained using the Argus instrument (Frayser et al. 2019) on the 100m Robert C. Byrd Green Bank Telescope (GBT) under project number GBT19B-182 on 2019 October 24, 25, and on 2019 November 14. Argus is a 16-pixel W-band array receiver, operating between 74 and 115 GHz. We observed the blazar J0319+4130 (3C84) every 30-50 min, depending on weather conditions, to obtain the pointing and focus solutions. We configured the Versatile GBT Astronomical Spectrometer (VEGA) backend to a rest frequency of 93,173.704 MHz, using mode 4 with 187.5 MHz bandwidth and a spectral resolution of 5.7 kHz. Science scans were obtained in on-the-fly (OTF) mapping mode and calibration scans were performed before and after each science block. The system temperatures are 110 K for all beams. The observations were carried out using frequency switching mode (frequency shift ± 12.5

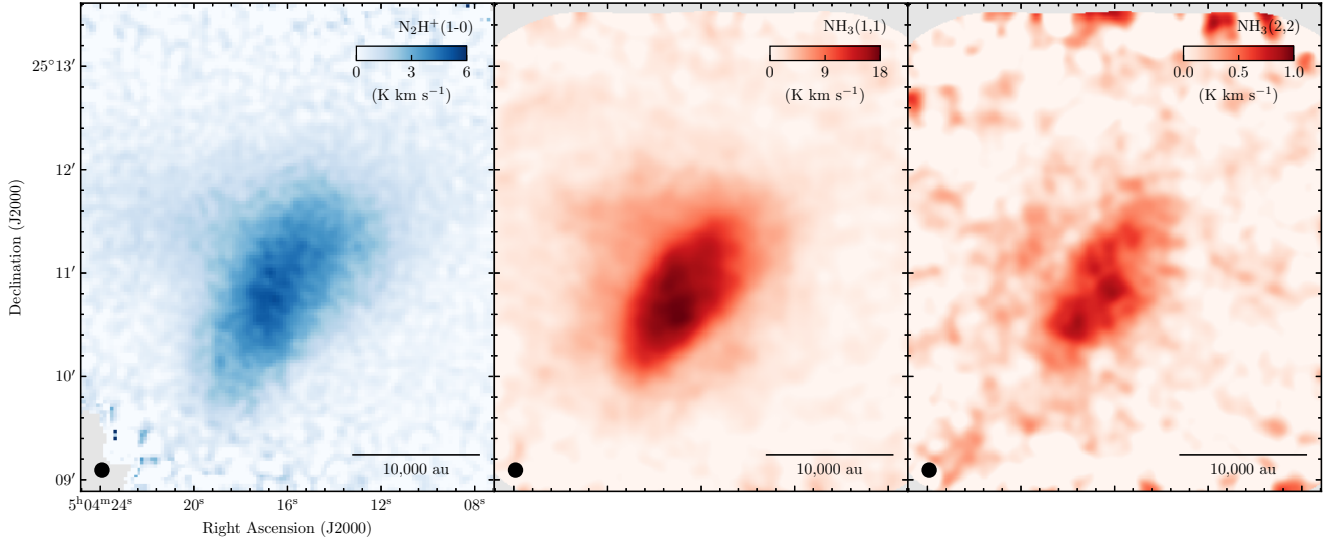


Figure 1. L1544 Integrated Intensity Maps. *Left:* $\text{N}_2\text{H}^+(1-0)$ *Middle:* $\text{NH}_3(1,1)$, *Right:* $\text{NH}_3(2,2)$. The beam size and the scale are denoted in the bottom left and right corners, respectively.

MHz). Standard calibration was performed using the GBTIDL package (Marganian et al. 2006) following the Argus appropriate procedures (Frayer et al. 2019). We mapped the calibrated data using the griddata task from the python-based gbtpipe¹ and applied a baseline subtraction by fitting a polynomial (blorder=5) to line-free channels prior to gridding the data. The integrated intensity map is calculated over all hyperfine components and shown in the left panel of Fig. 1. The spatial resolution is $7.81''$ and the spectral resolution is 0.018 km s^{-1} .

The $\text{NH}_3(1,1)$ and $\text{NH}_3(2,2)$ data were obtained with the Karl G. Jansky Very Large Array (VLA) under project number VLA19B-180 on 2019 November 18, 27, and on 2019 December 03, 19. Matching short-spacing observations of the same lines were obtained with the GBT under project number GBT19B-182 on 2019, December 7. The VLA data are a 10-point mosaic, which was imaged using multiscale clean and then combined with the single-dish data using the model image. The integrated intensity maps, calculated over all hyperfine components are shown in the middle and right panel of Fig. 1. The spatial resolution of the combined data cubes are $4.31'' \times 4.14''$, -77.2° and the spatial resolution is 0.066 km s^{-1} .

3. METHODS

3.1. SpectralCube

This project was my first introduction to radio astronomy so I began by learning spectral-cube² (Ginsburg et al. 2019). It is an incredibly powerful python package and I used it to manipulate the data cubes that I was given. I used it for the standard opening and gleaning data from the cube and header. I also used it to smooth the cubes. The spectral resolution of the N_2H^+ data is a factor of ~ 3.5 than that of the NH_3 data cubes, which meant that they needed to be smoothed so that they were comparable. In addition the spatial resolution of the VLA+GBT NH_3 data is intrinsically higher compared to the GBT/Argus N_2H^+ data cube. Both cubes were then smoothed to a common beam size of $8''$ and a spectral resolution of 0.07 km s^{-1} . In addition to smoothing the cubes, I used SpectralCube to regrid the cubes to a common pixel size.

3.2. PySpecKit

The next step in obtaining the line widths of each molecule was to fit the data. For this I used PySpecKit³ (Ginsburg & Mirocha 2011; Ginsburg et al. 2022).

3.2.1. N_2H^+

¹ <https://github.com/GBTSpectroscopy/gbtpipe>

² <https://github.com/radio-astro-tools/spectral-cube>

³ <https://github.com/pyspeckit/pyspeckit>

To fit N_2H^+ I used the `n2hp_vtau` model. The required parameter for the model are: Excitation temperature, T_{ex} ; optical thickness, τ ; line-of-sight velocity, v_{lsr} ; and velocity dispersion, σ . We assumed the data to be optically thin and hence set $\tau = 0.1$. The guesses that I gave the fit were $T_{\text{ex},0} = 5$ K, $v_{\text{lsr},0} = 7$ km s $^{-1}$ and $\sigma_0 = 0.1$ km s $^{-1}$. The fit took about two and half hours to run and it gave me 8 frames: the original parameters and their errors.

3.2.2. NH_3

I used `PySpecKit`'s cold ammonia model to simultaneously fit the $\text{NH}_3(1,1)$ and $\text{NH}_3(2,2)$ data cubes. This is a reasonable assumption, since the $\text{NH}_3(3,3)$ transition is, as expected, not detected in this core, indicating this is a cold source. The parameters of this model are: Kinetic temperature, T_{kin} ; excitation temperature, T_{ex} ; logarithmic NH_3 column density, $\log(N(\text{NH}_3))$; velocity dispersion, σ ; line-of-sight velocity, v_{lsr} ; and ortho-to-para ratio, $F(\text{ortho})$. I fixed the ortho-to-para ratio to 0.5. The initial guess that I provided for each of the other parameter were: `Tk.mean` (the mean kinetic temperature of the cube), $T_{\text{ex}} = 7$ K, $\log(N(\text{NH}_3)) = 14.5$, $\sigma = 0.15$ km s $^{-1}$. For the line-of-sight velocity I used the results from the moment 1 map.

3.3. `AplPy`

To plot the cubes I used `AplPy`⁴ (Robitaille & Bressert 2012; Robitaille 2019) for the first time. I found the program to be incredibly astronomer friendly and it was quite easy to plot data. The issue that I ran into was that it was not too friendly for radio astronomers who work with spectral-line data. I wanted to recenter the data in the plots so I went to use the `recenter` function. Using this function on my fitted cubes led me to a `WCSError`. I didn't find a perfect solution but a work around: I squeezed the data cubes and then separate the frames of the cube into their own fits files. This eventually worked for the better because I needed data from the individual frames and it was simpler to call individual files than slicing the cube.

4. RESULTS

4.1. *Fit and Error Maps*

Figure 2 shows results from the optically thin N_2H^+ fits in the top row and the corresponding error maps in the bottom row. The maps are mostly to be expected. Since the optical thickness, τ is fixed to 0.1 we omit the corresponding map as it yields no new information. The line-of sight-velocity, v_{lsr} is ~ 7 km s $^{-1}$, and velocity dispersion, σ is ~ 0.1 km s $^{-1}$. We note that the velocity dispersion maps indicated narrower line widths towards the center of the prestellar core compared to the edges of the map.

In Fig. 3 we show the fit results from the simultaneous fits of $\text{NH}_3(1,1)$ and $\text{NH}_3(2,2)$ in the top row and the corresponding error maps in the bottom row. This fit, once again, has expected values. The range of the kinetic temperature, T_{kin} is within a expected range of ~ 8 K for a prestellar core, the column density is relatively uniform, the velocity dispersion is ~ 0.1 km s $^{-1}$, and peak of the line-of-sight velocity is ~ 7 km s $^{-1}$.

4.2. *Velocity Dispersion and Sonic Mach Number*

Spectral lines can broaden because energy levels are not infinitely sharp. Molecules move and the temperature of gas can affect the random motions of these molecules which cause thermal broadening of the spectral line. Random turbulent motion also causes line broadening (or non-thermal line widths). I used the kinetic temperature from the NH_3 fitting to determine the thermal component of velocity dispersion and removed it from the fitted velocity dispersion to get the non-thermal component which is used in the final comparisons. I determine the non-thermal velocity dispersion, σ_{NT} , of the molecules as

$$\sigma_{\text{NT}}^2 = \sigma_v^2 - \sigma_{\text{th}}(T_{\text{kin}})^2, \quad (1)$$

where σ_v is the measured velocity dispersion, σ_{th} is the thermal velocity dispersion of the observed species,

$$\sigma_{\text{th}} = \sqrt{\frac{k_{\text{B}} T_{\text{kin}}}{\mu m_{\text{H}}}}, \quad (2)$$

where μ is the molecular weight of the observed species, m_{H} is the hydrogen mass, and k_{B} is Boltzmann's constant. I determine the level of non-thermal velocity dispersion, σ_{NT} for both molecules using the kinetic temperature measured from NH_3 and Eq. 1.

⁴ <https://github.com/aplpy/aplpy>

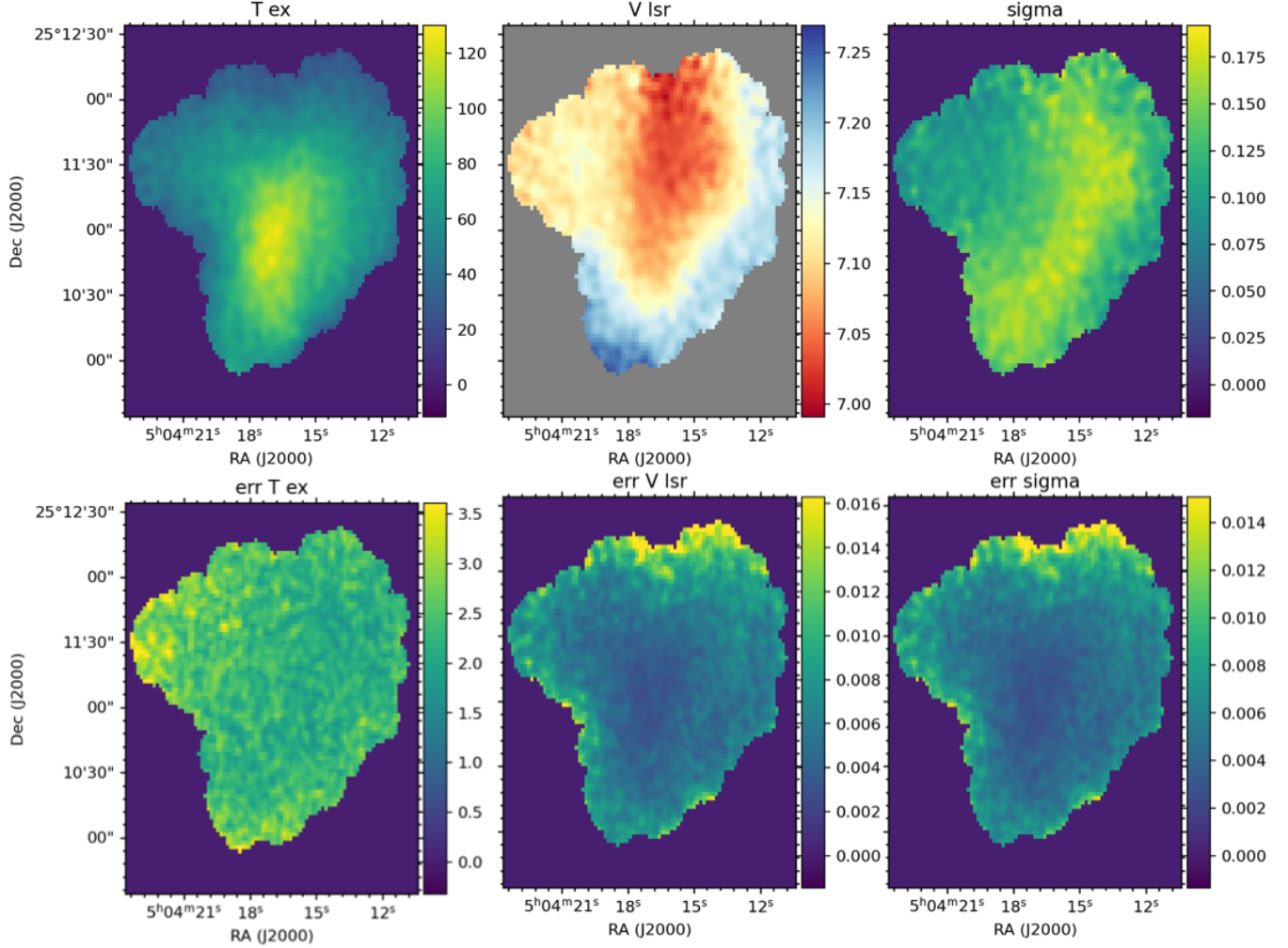


Figure 2. Fit results for the N_2H^+ data cube. *Top row:* Fitted parameters. *Bottom row:* Corresponding error maps. *From left to right:* Excitation temperature T_{ex} in units of Kelvin; line-of-sight velocity v_{lsr} in units of km s^{-1} ; and velocity dispersion in units of km s^{-1} .

I estimate the sonic Mach number, M , of the turbulence as

$$M = \frac{\sigma_{\text{NT}}}{c_s}, \quad (3)$$

where c_s is the sound speed of the mean particle (using Eq. 2 with $\mu=2.37$; Kauffmann et al. 2008).

In Fig. 4, I show the distribution of the sonic Mach number, M for the ion and the neutral. As Figure 4 shows, the ion, N_2H^+ , appears to have a slightly greater distribution than that of the neutral, NH_3 .

5. FUTURE WORK

In the future we want to correct some of the issues that arose when analyzing the maps that I plotted. One of the most glaring issues with the N_2H^+ fit is the excitation temperature. The top left map in Fig. 2 shows that it has temperatures ranging from 0 on the edges to 120K in the center. A possible explanation for this is that maybe we incorrectly assumed that the data is optically thin and by fixing the value, the fit needed to compensate for this somehow and hence increased the excitation temperature.

Another potential issue that we want to address is the structure of the N_2H^+ spectra. Due to their shape, we believe that it could possibly have two velocity components. When I smoothed the cube in the beginning we suspect that the second component was eliminated. Figure 5 zooms in on one of the hyperfine peaks. The red line is the original spectrum and the black line is the smoothed spectrum. There appear to be two independent peaks in the red

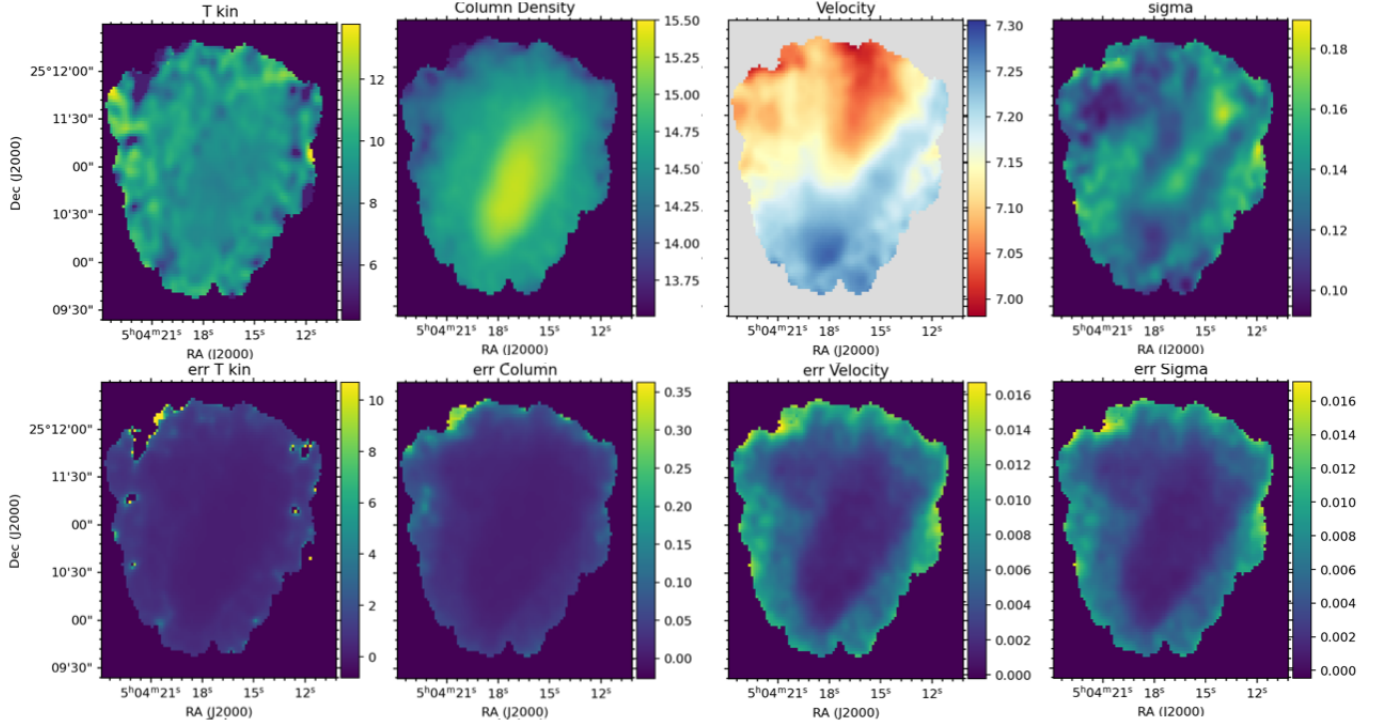


Figure 3. Fit results for the simultaneous fit of $\text{NH}_3(1,1)$ and $\text{NH}_3(2,2)$ data cubes. *Top row:* Fitted parameters. *Bottom row:* Corresponding error maps. *From left to right:* Kinetic temperature T_{kin} in units of Kelvin; column density in logarithmic units of cm^{-2} ; line-of-sight velocity v_{lsr} in units of km s^{-1} ; and velocity dispersion in units of km s^{-1} .

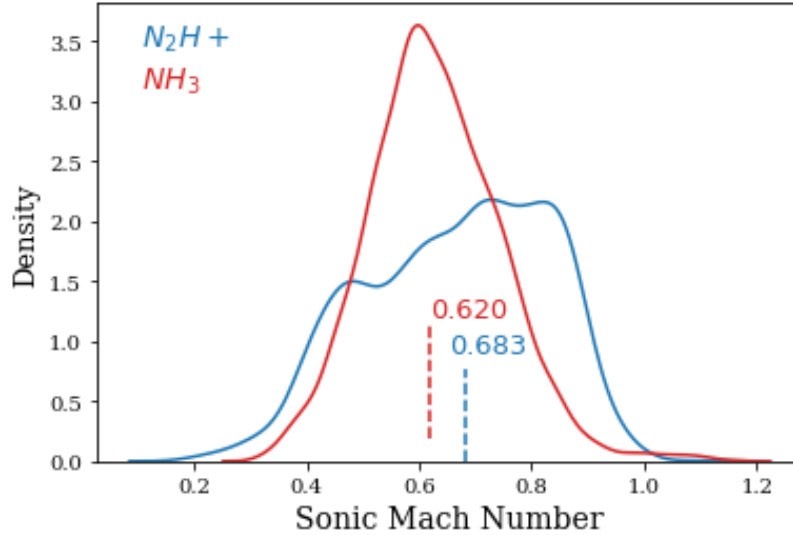


Figure 4. Distribution of the Sonic Mach Number M the ion N_2H^+ in blue and the neutral NH_3 in blue.

spectrum that got smoothed to a single peak in the black spectrum. If there were only a single velocity component along the line-of-sight, we would only expect to see a single peak. Two peaks could be indicative of the presence of a second velocity components. In the future we hope to investigate this further and if it does turn out to have multiple components then we will compare each component to the neutral molecule to hopefully get a more definitive answer.

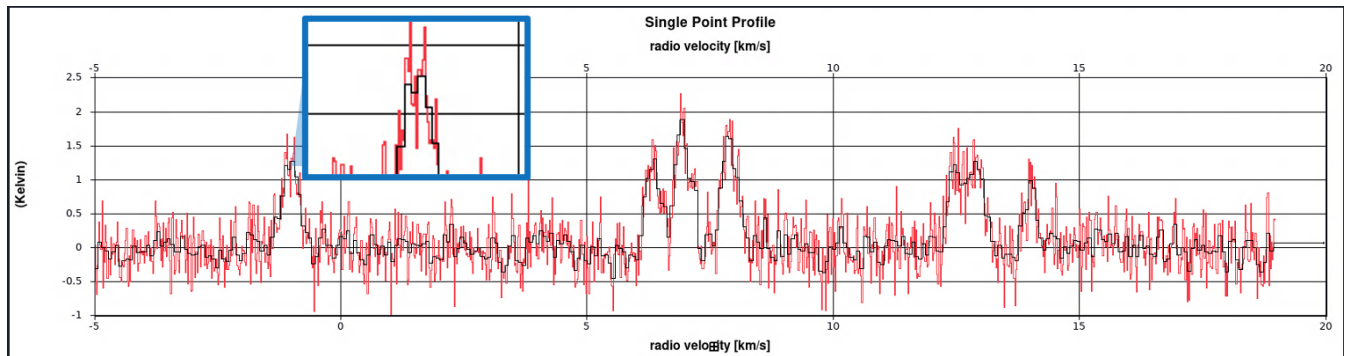


Figure 5. Comparison of a N_2H^+ spectrum of the unsmoothed data (spectral resolution of 0.018 km s^{-1}) in red and the smoothed data (spectral resolution of 0.07 km s^{-1}) in black.

Overall this was a very rewarding experience and I'm grateful for having worked for the observatory this past summer. It has solidified my passion for Radio Astronomy and I look forward to continuing this work in the future.

REFERENCES

- Frayer, D. T., Maddalena, R. J., White, S., et al. 2019, arXiv e-prints, arXiv:1906.02307
- Galli, P. A. B., Loinard, L., Ortiz-Léon, G. N., et al. 2018, ApJ, 859, 33
- Ginsburg, A., & Mirocha, J. 2011, PySpecKit: Python Spectroscopic Toolkit, Astrophysics Source Code Library, record ascl:1109.001. <http://ascl.net/1109.001>
- Ginsburg, A., Sokolov, V., de Val-Borro, M., et al. 2022, AJ, 163, 291
- Ginsburg, A., Koch, E., Robitaille, T., et al. 2019, radio-astro-tools/spectral-cube: Release v0.4.5, v0.4.5, Zenodo, Zenodo, doi: [10.5281/zenodo.3558614](https://doi.org/10.5281/zenodo.3558614)
- Kauffmann, J., Bertoldi, F., Bourke, T. L., Evans, N. J., I., & Lee, C. W. 2008, A&A, 487, 993
- Larson, R. B. 1981, MNRAS, 194, 809
- Marganian, P., Garwood, R. W., Braatz, J. A., Radziwill, N. M., & Maddalena, R. J. 2006, in Astronomical Society of the Pacific Conference Series, Vol. 351, Astronomical Data Analysis Software and Systems XV, ed. C. Gabriel, C. Arviset, D. Ponz, & S. Enrique, 512
- Pineda, J. E., Schmiedeke, A., Caselli, P., et al. 2021, ApJ, 912, 7
- Robitaille, T. 2019, APLpy v2.0: The Astronomical Plotting Library in Python, 2.0, Zenodo, Zenodo, doi: [10.5281/zenodo.2567476](https://doi.org/10.5281/zenodo.2567476)
- Robitaille, T., & Bressert, E. 2012, APLpy: Astronomical Plotting Library in Python, Astrophysics Source Code Library, record ascl:1208.017. <http://ascl.net/1208.017>
- Shirley, Y. L. 2015, PASP, 127, 299
- Sokolov, V., Wang, K., Pineda, J. E., et al. 2019, ApJ, 872, 30
- Solomon, P. M., & Rivolo, A. R. 1989, ApJ, 339, 919
- Tafalla, M., Myers, P. C., Caselli, P., & Walmsley, C. M. 2004, A&A, 416, 191
- Zucker, C., Schlafly, E. F., Speagle, J. S., et al. 2018, ApJ, 869, 83